ELSEVIER

Polymer 41 (2000) 3289–3295

polymer

Monte Carlo simulation of self-avoiding lattice chains subject to simple shear flow
Part II. Three-dimensional results and comparison with experiments

Guoqiang Xu[a], Jiandong Ding[a,*], Yuliang Yang[a,b]

[a]*Department of Macromolecular Science, Laboratory of Molecular Engineering of Polymers, Fudan University, Shanghai 200433, People's Republic of China*
[b]*Institute of Chemistry, Chinese Academy of Sciences, Beijing 100080, People's Republic of China*

Received 16 March 1999; accepted 16 June 1999

Abstract

This paper has extended a lattice Monte Carlo (MC) method to simulate the simple shear flow of multiple self-avoiding chains in three dimensions following our research work in two dimensions. Comparisons of simulation outputs with experimental observations, theoretical predictions and other simulation results are made. The steady-state scaling analysis to scattering functions of deformed chains confirms the existence of anisotropic scaling laws at fixed reduced shear rates found in molecular dynamics (MD) simulation. The exponent of chain deformation shown in the MC simulation falls into a normal regime measured from neutron scattering and light scattering experiments. The relation between orientation angles and shear rates is consistent with some scattering experiments. Both Newtonian and non-Newtonian regimes are reproduced in our lattice MC simulation. Non-zero first and second normal stress differences and their dependence of the shear rate are found, as well as the shear thinning effect. The stress growth at inception and stress decay after cessation of shear flow is also examined. The validity of our novel simulation approach is thus confirmed. Since both chain conformations and rheological properties under shear flow can be studied, our MC approach can be used to reveal non-linear viscoelasticity of polymer fluids and polymer-flow interaction.

Keywords: Monte Carlo simulation; Simple shear flow; Thinning effect

1. Introduction

Chain deformation in flow field is a classic problem [1–3] and now becomes one of the hot topics [4–6] in polymer science. Computer simulation or computer experiment constitutes the third research approach besides theory and experiment [7], with the advantages that the non-linear dynamics can be dealt with. Molecular dynamics (MD) simulation [8,9], Brownian dynamics simulation [10–12] and off-lattice MC simulation [13–17] have been successfully used to simulate chain deformation in shear flow. Especially, a wonderful scaling analysis of chain conformation under shear has been performed by Pierleoni and Rychaert [8,9] using MD simulation, and was found in good agreement with the small angle neutron scattering (SANS) experiment by Lindner and Oberthur [18,19]. However, the rheological behaviors have not been studied [8,9] and thus the relationship between chain deformation and non-linear viscoelasticity of polymers cannot be elucidated.

Lai and Binder [20] and Lai and Lai [21] also have treated the endgrafted polymers in shear flow with the lattice Monte Carlo (MC) simulation extensively by changing the jump rate in the flow direction thus associated with the velocity profile. However, in our lattice MC method of simple shear flow, a pseudo-potential describing the flow field has been introduced, which has been extended to simulate the flexible chains in two dimensions [22] and successfully applied to study anisotropic and enhanced two-dimensional self-diffusion of a chain under shear flow [23]. In this paper the lattice MC method will be used to simulate the simple shear flow of self-avoiding lattice chains in three dimensions, by which the validity of this novel formalism is further confirmed by comparison with present theories, experiments and other simulations. Our improvement of the lattice MC simulation algorithm is much helpful for studies of non-linear rheological behaviors of multi-chain systems. The advantage of our novel method is that macroscopic stresses can be obtained by statistics of sampled

* Corresponding author. Tel.: +86-21-65642863; fax: +86-21-65640293.
E-mail address: ylyang@srcap.stc.sh.cn (Y. Yang).

0032-3861/00/$ - see front matter
PII: S0032-3861(99)00492-9

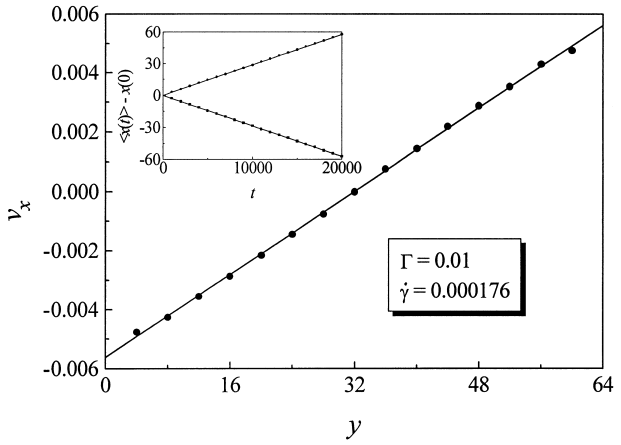

Fig. 1. Simulated flow velocities at different positions along the dimension of the velocity gradient. The inserted plot indicates the mean displacement along the flow direction $\langle x(t)\rangle - x(0)$ as a function of the MC time t. (For every point, the statistics is performed in the steady state at a given shear rate after evolution for 500,000 MC cycles from the initial state to get the equilibrium state; the ensemble average over 20 independent runs is performed and for each run, the time average over 20,000 MC cycles is made. The system size is $64\times64\times64$, $n_p = 100$, $N = 40$, $\varphi = 0.122$.)

configuration distribution function (CDF). The rheological behaviors of a semi-dilute polymer solution are studied together with scaling analysis in this paper by MC simulation. The non-linear viscoelasticity is closely related to chain deformation.

2. Model and velocity profile of simulated flow field

It is relatively difficult to introduce the flow potential in lattice MC simulation, so this method has not been used into flow process until our last paper was published, although the Kramers potential flow [24] has been successfully simulated earlier [25]. The key in our MC simulation under simple shear flow is that we introduce a pseudo-potential of shear flow which makes sense only for the *potential difference* associated with MC sampling for every local movement of a bead in the lattice chain *strictly defined by the bond fluctuation algorithm*, which has been applied to deal with many problems of chain conformation and chain dynamics in zero field [26–30]. This algorithm was proposed by Carmesin and Kremer [26] originally in two dimensions, and then developed into three dimensions by Deutsch and Binder [28] and Wittmann et al. [29]. The simulation approach of simple shear flow of lattice chains is similar to that in two dimensions [22,23]. Our pseudo-potential should be associated with the elementary move of a bead between two points (x,y,z) and $(x+\Delta x, y+\Delta y, z+\Delta z)$. Here, the x, y and z directions are defined as the flow, velocity gradient and vortex directions, respectively. In the bond-fluctuation algorithm based on cubic lattices, Δx, Δy, Δz can take value -1, 0 or 1 and only one of them can be non-zero for each elementary move. The potential difference for an elementary move is written as

$$\Delta U_s = \begin{cases} 0 & (\Delta y \text{ or } \Delta z = \pm 1) \\ \mp \mathrm{k}T\Gamma y & (\Delta x = \pm 1) \end{cases} \quad (1)$$

Since a bond of a self-avoiding chain corresponds physically to a "Kuhn segment", a harmonic elastic energy associated with the bond fluctuation is introduced by us in the form of

$$U_{el} = \tfrac{1}{2}\mathrm{k}TKl^2 \quad (2)$$

In three dimensions, bond lengths are taken as 2, $\sqrt{5}$, $\sqrt{6}$, 3, or $\sqrt{10}$ to avoid intersection of chain segments whereas bond angles can be altered within 87 values [28]. So, the spring is somewhat similar to the Tanner spring [31] or a "linear locked" spring with the restriction of $l_{min} \le l \le l_{max}$.

All data in this paper result from Glauber dynamics sampling [32] with the acceptance probability of each tried elementary move as

$$P = \frac{\exp[-\Delta E/(\mathrm{k}T)]}{1+\exp[-\Delta E/(\mathrm{k}T)]} \quad (3)$$

The transition probabilities involve an energy change ΔE between the new (trial) and the old states. A linear velocity gradient can be achieved in our lattice MC simulation based on the pseudo-potential unless the shear rate is unreasonably high such as $\Gamma y > 1$. Since the Glauber dynamics simulation results in broader linear range of shear rate [22,23], we prefer this sampling method to the conventional Metropolis importance sampling [33].

The MC simulation is performed on $64\times64\times64$ cubic lattices. The periodic boundary condition is employed along the x and z directions whereas two hard walls are set along the y direction. A semi-dilute polymer solution with the occupied volume fraction $\varphi = 0.122$ is examined in detail with the number of segments per chain $N = 40$ and the number of polymeric chains $n_p = 100$ unless otherwise indicated.

The steady velocity at any fixed y position has been achieved by our novel MC method, which can be seen from the linear relation in the inserted plot of Fig. 1. The slope of the corresponding fitted straight line gives the corresponding velocity $v_x(y)$. So a linear velocity gradient along the y direction is achieved, which clearly demonstrates that the simulated velocity profiles satisfy the requirements of simple shear flow. The simulated shear rate $\dot\gamma$ in the unit of t_{MC}^{-1} (t_{MC} is the MC step) is obtained from the slope of the corresponding fitted straight line and is different from the inputted reduced shear rate Γ in the unit of l_{MC}^{-2} (l_{MC} is the unit lattice size).

3. Steady-state scaling analysis for chains under shear

Using the above MC method, the configuration of multiple self-avoided chains under simple shear flow can be easily studied in three dimensions. The chain shape is

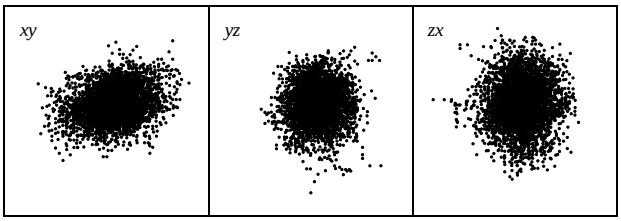

Fig. 2. Steady-state chain shape under simple shear flow at $\Gamma = 0.002$ illustrated by projection of 100 plane multi-chain configurations on the three indicated cross-sections. Before projection, the centers of mass of the 100 chains have been moved to the same point.

graphically illustrated in Fig. 2, according to which, the chains are elongated along the flow direction while contracted along the velocity gradient direction with the normal dimension almost kept unchanged.

The chain structure over the whole range of relevant length scales can be reflected by the static structure factor defined as [8,9,27]

$$S(\boldsymbol{k}) = \frac{1}{N}\sum_{i,j=1}^{N}\langle \exp[-\boldsymbol{k}\cdot(\boldsymbol{r}_i - \boldsymbol{r}_j)]\rangle \tag{4}$$

where $\boldsymbol{r}_i$ is the segment coordination, $\boldsymbol{k}$ the scattering vector, and $\langle\cdots\rangle$ indicates ensemble average. The intermediate-k regime affords information on the spatial correlation of segments.

It has been noted by Pierleoni and Ryckaert [8,9] that a universal anisotropic scaling law exists for deformed chains with different chain lengths, if the reduced shear rate β is fixed. β is physically related to the apparent shear rate as $\beta = \dot{\gamma}\tau_N$, where τ_N is the longest relaxation time of the polymer with N segments, here it is determined by the mode-correlation method for Rouse chains at equilibrium, just following Carmesin and Kremer [27]. The structure factors of chains in different chain lengths are compared under the same reduced shear rate (Fig. 3). The anisotropic

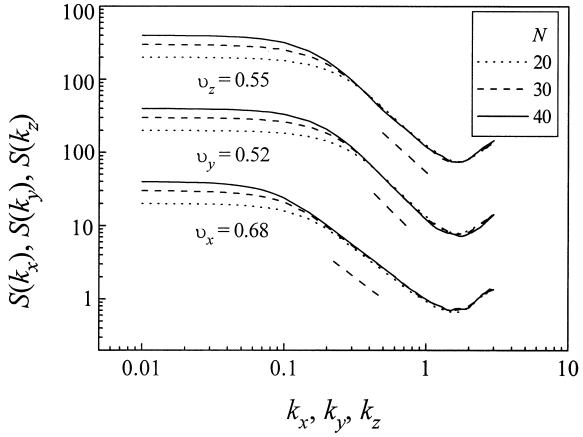

Fig. 3. Structure factors of chains with different chain lengths under shear at the fixed reduced shear rate β. For the chains with $N = 20$, 30 and 40, n_p and Γ are increased to keep φ and β unchanged, respectively. (The other parameters are the same as those in Fig. 1.)

scaling law put forward by the MD simulation of a single chain [8,9] is thus confirmed by our lattice MC simulation in multi-chain systems. The static scaling exponent υ can be obtained from the slope of the fitted line $(-1/\upsilon)$. At equilibrium, $\upsilon = 0.55$ for this semi-dilute solution, which is reasonably between 0.5 for a very concentrated solution and 0.58 for a very dilute solution [34]. Subjected to simple shear flow, υ_x gets increased, υ_y becomes decreased while υ_z is almost kept unchanged, which is in accord with the flow-induced anisotropic change of chain shapes (Fig. 2). The above change agrees with the measurement from scattering experiment [18,19] and also with the statistics from MD simulation [8,9].

4. Chain stretching and orientation under simple shear flow

The chain size and shape can be described by the radius of gyration tensor

$$\hat{\boldsymbol{S}}^2 = \frac{1}{2N^2}\sum_{i,j=1}^{N}\langle(\boldsymbol{r}_i - \boldsymbol{r}_j)(\boldsymbol{r}_i - \boldsymbol{r}_j)\rangle \tag{5}$$

The mean square radius of gyration and the orientation angle with respect to the form birefringence can be obtained from [3]

$$S_G^2 = \mathrm{Tr}\,\hat{\boldsymbol{S}}^2 = S_x^2 + S_y^2 + S_z^2, \qquad \mathrm{tg}\,2\Theta = \frac{2S_{xy}}{S_x^2 - S_y^2} \tag{6}$$

Here, S_x^2, S_y^2 and S_z^2 also mean the x, y and z components of the scaled radius of gyration. On the other hand, the intrinsic birefringence can be described by the segment orientation tensor

$$\hat{P} = \left\langle \frac{\sum_{i=1}^{N-1}(\boldsymbol{r}_{i+1} - \boldsymbol{r}_i)(\boldsymbol{r}_{i+1} - \boldsymbol{r}_i)}{\sum_{i=1}^{N-1}|\boldsymbol{r}_{i+1} - \boldsymbol{r}_i|^2} - \frac{1}{3}\hat{\imath} \right\rangle \tag{7}$$

where $\hat{\imath}$ is the unit tensor. The orientation angle with respect to the segment orientation or the intrinsic birefringence can be obtained from Ref. [3]

$$\mathrm{tg}\,2\theta_{\mathrm{seg}} = \frac{2P_{xy}}{P_{xx} - P_{yy}} \tag{8}$$

The chain stretching is seen from the curve of chain size versus shear rate (Fig. 4). The chain size along the flow direction is increased, which leads to the increase of the global radius of gyration, while that along the velocity gradient is decreased. In theory, chains are not influenced along the vortex or normal direction. However, the size along the z direction is still found to decrease slightly if the chain stretching is very striking under high shear rates.

The scaling law of chain deformation has earlier been predicted by the dynamic chain models expressed as

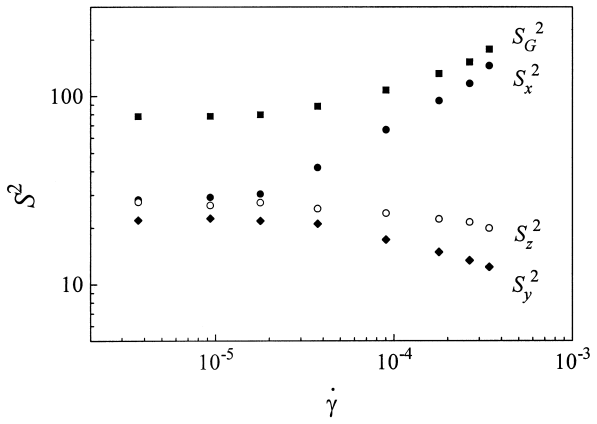

Fig. 4. Mean square radius of gyration, S_G^2 along with its *x*, *y* and *z* components as a function of shear rate $\dot{\gamma}$.

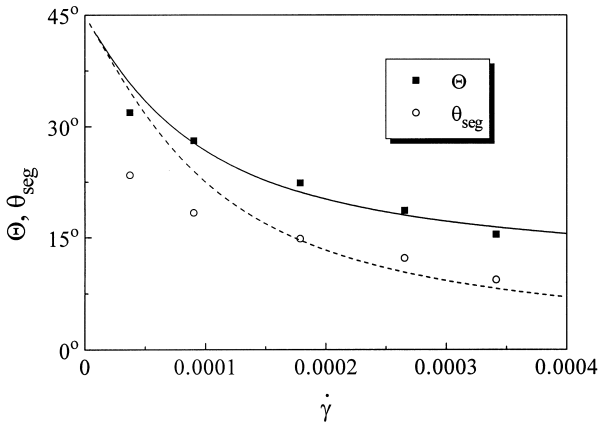

Fig. 6. Averaged orientation angles Θ and θ_{seg} as a function of shear rate $\dot{\gamma}$. The dashed and solid lines are the theoretical results from Eqs. (10) and (11) with $\Theta = 0.5 \arctan(0.0001/\dot{\gamma})$ and $\Theta = 0.5 \arctan[(0.0001/\dot{\gamma}) + 0.35]$.

[35–37]

$$S_G^2/S_0^2 - 1 \sim \beta^{\alpha} \tag{9}$$

where S_0^2 is the mean square radius of gyration at equilibrium state. α is said to be 2 according to Rouse model (bead-spring model) [35], Zimm model (bead-spring model including hydrodynamic interaction) [36] and Kuhn model (elastic dumbbell model) [37]. The simulated chain deformation is, however, smaller than that predicted in theory (Fig. 5). Lindner and Oberthur studied the conformation of polystyrene (PS) in a dilute solution under a constant shear gradient with SANS. Although a satisfactory agreement is found at low β ($\beta < 1$), the trend of the increase of the chain deformation is strikingly weak at high shear rates ([15, Fig. 10; 16, Fig. 3]). Link and Springer reported $\alpha =$ 1.4 in their laser light scattering (LS) experiment of PS ([35, Fig. 11 and Eq. (13)]). A similar phenomenon was observed by Cottrell et al. [39] and even lower deformation was described with, according to the calculation of Link and Springer, $\alpha = 1.03$. Our simulation is, therefore, semi-

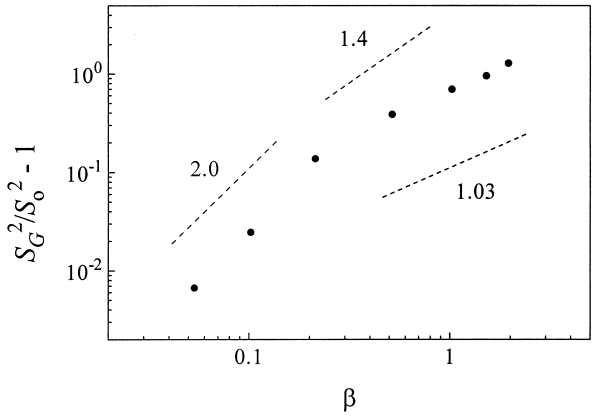

Fig. 5. The deformation ratio of chains under shear flow ($S_G^2/S_0^2 - 1$)as a function of reduced shear rate β. (Slope = 2.0 predicted by Rouse, Zimm or Kuhn dynamics theory, while slope = 1.4 and 1.03 resulting from LS experiments in Refs. [31] and [30], respectively.)

quantitatively coincident with the experimental observations. The deviation from theory at high shear rate may be easily accounted for from the fact that chain conformations under shear are still assumed to be Gaussian in theory, which is neither true in simulation nor in experiment especially in the non-linear regime.

In the rheo-optical experiment, the flow birefringence is usually the combination of the intrinsic birefringence and the form birefringence. It is easy to distinguish them in computer simulation. The orientation angles with respect to both the intrinsic birefringence and form birefringence are plotted in Fig. 6. The two sorts of orientation angles are different from each other. Therefore, the deformation of the global flexible coils under simple shear flow does not take place with the segment orientation strictly simultaneously. As far as the form birefringence is concerned, the orientation angle can be determined from scattering experiment. In theory, the ideal Rouse model [35] predicts, along with Zimm model [36] and Kuhn model [37], that

$$\Theta = \tfrac{1}{2} \arctan(b/\beta) \tag{10}$$

where b is a positive constant. This formula implies that $\Theta \to \pi/4$ when $\beta \to 0$, and $\Theta \to 0$ when $\beta \to \infty$. The main difference between the present theories and our simulation is that the asymptotic orientation angle of flexible polymers might not be zero with shear rate increased infinitely (Fig. 6), just similar to rigid molecules [40]. A similar phenomenon has been observed in scattering experiment of polystyrene in shear flow by Link and Springer [38]. A revised formula has been put forward by them as

$$\Theta = \tfrac{1}{2} \arctan\left(\frac{b}{\beta} + c\right) \qquad (b, c > 0) \tag{11}$$

Our simulation outputs agree with Eq. (11) more than with Eq. (10). The main reason may lie in the fact that our simulated bead-spring model is self-avoided and can be used to describe the non-linear regime at high shear rates.

5. Shear rate dependence of rheological behaviors

The main privilege of our novel simulation approach is that we cannot only describe the microscopic chain conformation, but also determine the macroscopic stress independently by statistics of sampled CDFs. The non-linear rheological behaviors in multi-chain systems can be reproduced, and the relation between macroscopic stress and microscopic chain deformation can be elucidated.

The details of derivation of the statistical formula of stress was given in our previous paper [22]. After neglecting hydrodynamic interaction, the stress tensor is, following the Kramers form for the stress tensor of the bead-spring model [3], expressed as

$$\hat{\sigma} = \frac{\hat{\tau} - \hat{\tau}_0}{kT} = \frac{n_p}{V}\left[(N-1)\hat{\imath} - K\left\langle \sum_{i=1}^{N-1} (\boldsymbol{r}_{i+1} - \boldsymbol{r}_i)(\boldsymbol{r}_{i+1} - \boldsymbol{r}_i)\right\rangle\right] \quad (12)$$

in the unit of V_{MC}^{-1}, where V_{MC} is the volume in MC simulation. Here, $\hat{\tau}$ and $\hat{\tau}_0$ are the total stress tensor of polymer solution and that of pure solvent. The excluded volume effect on the macroscopic stresses [41,42] is inherently involved in the present statistic approach since the CDF has been influenced by this effect in our simulation.

The reduced first and second normal stress differences are expressed as

$$N_1 = \sigma_{xx} - \sigma_{yy}, \qquad N_2 = \sigma_{yy} - \sigma_{zz} \quad (13)$$

while the reduced apparent viscosity can be obtained from the reduced shear stress

$$\eta = \frac{\sigma_{xy}}{\dot{\gamma}} \quad (14)$$

The corresponding simulation outputs are shown in Fig. 7. Besides the shear stress, the normal stress differences are also reproduced and exhibit shear rate dependence for our free-draining bead-spring model with excluded volume effect. It is consistent with the experimental observations very well [1,43,44]. N_1 is positive and even larger than shear stress at high shear rates while N_2 is negative and very small. It seems worthwhile mentioning that the original Rouse model and most of other conventional models about chain dynamics and linear viscoelasticity fail to predict the non-linear change of normal stress differences with shear rate, and some classic theories even fail to predict non-zero second normal stress difference [1–3]. The comparison between the microscopic chain conformation (Fig. 4) and the complicated macroscopic rheological behaviors (Fig. 7) demonstrates that the non-zero normal stress difference in the non-Newtonian regime and thus the so-called elastic effect in polymer processing [43,44] originate essentially from anisotropic chain deformation.

The viscosity exhibits strong shear rate dependence, and the shear thinning effect at high shear rates widely observed

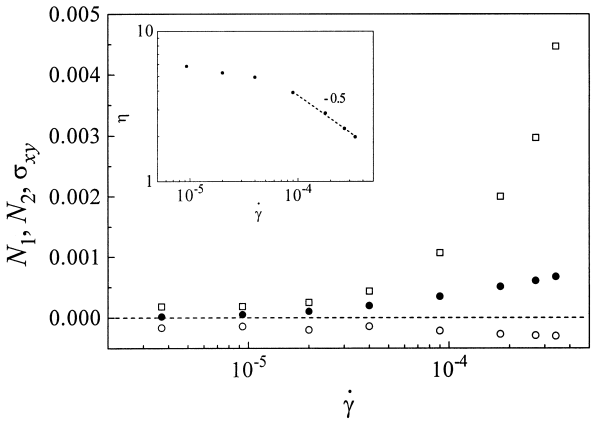

Fig. 7. Reduced shear stress σ_{xy} (●), first normal stress difference N_1 (□) and second normal stress difference N_2 (○) as a function of shear rate $\dot{\gamma}$. The inserted plot indicates the reduced apparent viscosity η as a function of shear rate $\dot{\gamma}$ and the fitted dashed line indicates the result of $\eta \propto \dot{\gamma}^{-0.5}$.

in experiment [1,43,44] is reproduced in our computer simulation. Therefore, we can obtain the material functions of flexible macromolecular chains subject to simple shear flow in both the Newtonian and non-Newtonian regimes. Many rheological experiments show that some scaling laws about shear rate dependence of viscometric functions exist in polymers under shear [1,43,44]. A power law can be expressed as

$$\eta \propto \dot{\gamma}^{n-1} \quad (15)$$

Obviously, $n = 1$ leads to the Newtonian fluid. If $n < 1$, the fluid is said to be "pseudoplastic" while $n > 1$ refers to "dilatant fluids". Most of polymeric fluids are pseudo-plastic with $0.2 < n < 0.7$ in common [1]. The power law is observed in our MC simulation at high shear rates within some ranges with a reasonable scaling exponent $n = 0.5$. So, our lattice MC simulation agrees with many experimental measurements even semi-quantitatively.

6. Dynamics of stress growth and stress decay

Non-linear rheological behaviors are also reflected in the dynamics from one state to another state such as in start-up dynamics. Corresponding studies are meaningful for polymer processing [43,44]. The stress growth at inception of shear flow is shown in Fig. 8 along with the stress decay after cessation of shear flow. An overshoot of stresses in the start-up dynamics occurs, which is well known in experiments [1,43,44]. Different from the start-up dynamics of liquid crystalline polymers, where the overshoots are pronounced at low shear rates but are suppressed at high shear rates [40], that of flexible polymers exhibits overshoots at high shear rates over a critical value [1,43–45]. This complicated experimental rheological behavior has been reproduced in our MC simulation. Our simulation indicates that the position of overshoot peak shifts to higher

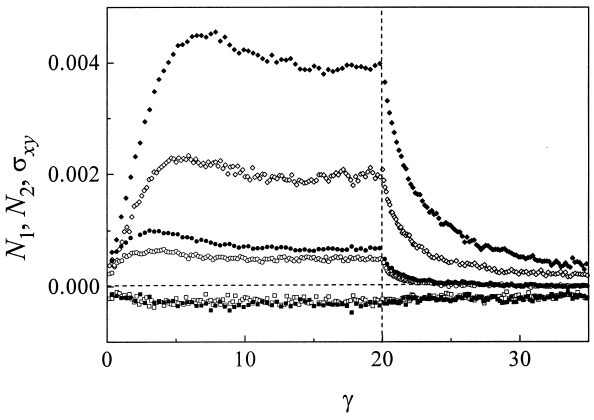

Fig. 8. Change of macroscopic stress and normal stress differences vs. shear strain at inception of and after cessation of shear flow. (open symbol: $\Gamma = 0.01$, solid symbol: $\Gamma = 0.02$, diamond symbol: N_1, square symbol: N_2, cycle symbol: σ. The shear strain after cessation of shear flow is also obtained from $\gamma = \dot{\gamma}\, t$).

shear strain γ while smaller in terms of shear time t with increase of shear rates. This result agrees with experimental observations of flexible polymers very well [1,43–45] although the critical shear rate over which the overshoot appears is strongly dependent upon the relaxation time, which is, in turn, dependent upon the chain density very much. Even the concrete values of the peak positions, namely, several shear strains are in the similar order of experimental measurements of most flexible polymers [1], which also demonstrates that our novel simulation approach of the shear flow of self-avoiding lattice chains can be applied to study the non-Newtonian rheological behaviors of polymers semi-quantitatively. The stress decay is meanwhile observed and the relaxation rates associated with high shear rates are faster than those with low shear rates, which agrees with experiments [1,43–45]. One has seen that the chain coils are highly stretched, i.e. stored more entropy elastic energy, when the shear rate is high, which results in faster stress relaxation.

7. Conclusions

This paper has, for the first time, extended the lattice MC method to simulate the simple shear flow of self-avoiding chains in three dimensions. The key point of our improvement is that we have successfully designed a pseudo-potential describing the shear flow field which makes sense only for the potential difference associated with the elementary MC move strictly defined by the bond-fluctuation approach. Based on this novel MC method, the linear velocity gradient has been achieved and the requirements of simple shear flow are satisfied. All statistical quantities are obtained from the sampled CDFs under shear which are, although the corresponding analytical expression is unknown at the present time, influenced by the chainlike characteristics of polymers, excluded volume effect, etc. The hydrodynamics effect [46] is, however, not involved.

The great advantage of our approach is that both chain conformation and rheological properties in the non-Newtonian regime can be studied. The steady-state scaling analysis to scattering functions of deformed chains under shear flow confirms the existence of anisotropic scaling laws at fixed reduced shear rates. Self-avoiding chains are stretched and oriented under simple shear flow. However, the deformation ratios deviate from theoretical predictions at high shear rates although agreement is found at low shear rates. The deformation exponent at high shear rates falls into a normal regime measured from SANS and LS experiments. The orientation angles associated with the form birefringence are closely related with shear rates. The relation is, however, slightly different from that predicted by Rouse theory, but consistent with some experimental observations. The stress tensor is obtained by statistics of sampled CDFs. Non-zero first and second normal stress differences and their shear-rate dependence are reproduced, which is conventional for commercial polymers. Both Newtonian and non-Newtonian regimes are found in our MC simulation. Shear thinning effect is reproduced in the non-Newtonian regime with a reasonable power exponent widely observed in most of the polymers. An overshoot at start-up dynamics of shear flow is observed in our computer experiment. Similar agreement is found in the examination of the exponential stress decay after cessation of shear flow. The regularity shown in our MC simulation is in accord with that observed in experiments rather well. What is more, all the stress evolutions are accompanied with conformation change and chain dynamics. The relation between non-linear rheological behaviors and chain conformation under shear flow is thus revealed by our novel MC simulation. We reasonably promise that this approach can be further improved and applied to many studies associated with polymer-flow interaction.

Acknowledgements

This research was supported by NSF of China, The Doctoral Programme Foundation of Institution High Education from the State Education Commission of China, and The National Key Projects for Fundamental Research “Macromolecular Condensed State” from The State Science and Technology Commission of China.

References

[1] Bird RB, Hassager O, Armstrong RC, Curtiss CF. Dynamics of polymeric liquids, New York: Wiley, 1977.
[2] de Gennes PG. Scaling concepts in polymer physics, Ithaca, NY: Cornell University Press, 1979.
[3] Doi M, Edwards SF. The theory of polymer dynamics, Oxford: Clarendon Press, 1986.
[4] de Gennes PG. Science 1997;276:1999.

[5] Perkins TT, Smith DE, Chu S. Science 1997;276:2016.
[6] Bossart J, Ottinger HC. Macromolecules 1997;30:5527.
[7] Kremer K, Binder K. Comput Phys Rep 1988;7:259.
[8] Pierleoni C, Ryckaert JP. Phys Rev Lett 1993;71:1724.
[9] Pierleoni C, Ryckaert JP. Macromolecules 1995;28:5097.
[10] Liu TW. J Chem Phys 1989;90:5826.
[11] Dotson PJ. J Chem Phys 1983;79:5730.
[12] Ottinger HC. J Chem Phys 1986;84:1850.
[13] Biller P, Petruccione F. J Chem Phys 1988;89:2412.
[14] Biller P, Petruccione F. J Chem Phys 1990;92:6322.
[15] Groot RD, Agterof WGM. J Chem Phys 1994;100:1657.
[16] Duering E, Rabin Y. Macromolecules 1990;23:2232.
[17] Duering E, Rabin Y. Macromolecules. J Rheol 1991;35:213.
[18] Lindner P, Oberthur RC. Coloid Polym Sci 1988;266:886.
[19] Lindner P, Oberthur RC. Physica B 1989;156, 157:410.
[20] Lai P, Binder K. J Chem Phys 1993;98:2366.
[21] Lai P, Lai C. Phys Rev E 1996;54:6958.
[22] Xu G, Ding J, Yang Y. J Chem Phys 1997;107:4070.
[23] Xu G, Ding J, Yang Y. Macromol Theory Simul 1998;7:129.
[24] Kramers HA. J Chem Phys 1946;14:415.
[25] Frisch HL, Pistoor N, Sariban A, Binder K, Fesjian S. J Chem Phys 1988;89:5194.
[26] Carmesin I, Kremer K. Macromolecules 1988;21:2819.
[27] Carmesin I, Kremer K. J Phys (France) 1990;51:915.
[28] Deutsch HP, Binder K. J Chem Phys 1991;94:2294.
[29] Wittmann HP, Kremer K, Binder K. J Chem Phys 1992;96:6291.
[30] Wittmer HP, Paul W, Binder K. Macromolecules 1992;25:7211.
[31] Tanner RI, Stehrenberger J. J Chem Phys 1971;55:1958.
[32] Glauber RJ. J Math Phys 1963;4:294.
[33] Metropolis N, Rosenbluth AW, Rosenbluth MN, Teller AH, Teller E. J Chem Phys 1953;21:1087.
[34] Flory PJ. Principles of polymer chemistry, Ithaca: Cornell University Press, 1953.
[35] Rouse PE. J Chem Phys 1953;21:1272.
[36] Zimm BH. J Chem Phys 1956;24:269.
[37] Kuhn W. Kolloid-Z 1934;68:2.
[38] Link A, Springer J. Macromolecules 1993;26:464.
[39] Cottrell FR, Merrill EW, Smith KA. J Polym Sci A 1969;27:1415.
[40] Ding J, Yang Y. Rheol Acta 1994;33:405.
[41] Fixman M. J Chem Phys 1991;95:1410.
[42] Gao J, Weiner JH. Macromolecules 1992;25:3462.
[43] Han CD. Rheology in polymer processing, New York: Academic Press, 1976.
[44] Ferry JD. Viscoelastic properties of polymers, New York: Wiley, 1970.
[45] Klucker R, Candau F, Schosseler F. Macromolecules 1995;28:6416.
[46] Fixman M. J Chem Phys 1983;78:1594.